Isotropic−Cubic Liquid Crystalline Phase Transition in Aqueous Solutions of PLPC

Valeria Castelletto*

Ecole Normale Superieure, Laboratoire de Physique Statistique, 24 rue Lhomond, 75231 Paris Cedex 05, France

Lia Q. Amaral

Instituto de Física, Universidade de São Paulo, Caixa Postal 66318, CEP 05315-970, São Paulo, SP, Brazil

Received: June 11, 1999

The isotropic (I)−cubic (Q^{223}) phase transition is studied in micellar aqueous solutions of palmitoyllysophosphatidylcholine (PLPC), using X-ray scattering. A mechanism to describe the I−Q^{223} phase transition is proposed in terms of the local order in the concentrated I phase and of the long-range order in the lower concentration limit of the Q^{223} phase. Information on the micellar shape in the concentrated I phase, previously obtained by us, and in the Q^{223} phase, now obtained, together with previous NMR and X-ray diffraction results of the literature, are used in our analysis. It is found that a local cubic order already exists in the concentrated I phase, but the positional correlation is between clusters with 5 micelles. The measured distance between these clusters is equal to the distance between micelles centered in one of the special positions of the cubic structure of phase Q^{223} (which has 8 micelles in the unit cell with 2 special positions). The total micellar volume in the Q^{223} phase is compatible with micelles of same paraffinic volume as those already studied in the I phase.

I. Introduction

The phase diagram of palmitoyllysophosphatidylcholine (PLPC)/water system presents isotropic (I)−cubic (Q^{223})−hexagonal (H) phase transitions with increasing PLPC concentration.[1] The Q^{223} phase was observed in several amphiphile/water systems.[2−4] Its presence between the I and the H phases depends on the acyl chain length, existing for C12, C14, and C16 but not for C18 lysophosphatidylcholines,[1,5] that present direct I−H phase transitions as most single chain amphiphiles do.

The phase Q^{223} is a micellar cubic phase, made of discrete closed aggregates, and it must not be included in the set of bicontinuous cubic phases observed at lower water contents in systems containing surfactants and biological lipids, usually situated between H and lamellar (L) phases. Its basic structure is now well established by NMR[5,6] and X-ray[7,8] results, in agreement with a model proposed by Fontell,[9] with two different categories of closed aggregates (6 in one special position and 2 in the other). Such a model,[9] proposed to reconcile NMR data on diffusion and X-ray data on the primitive unit cell dimensions, was based on the known structure on solid γ-O_2, β-F_2, and N_2, of the same space group $Pm3n$, with micelles replacing the positions of the diatomic molecules.

The model given by Fontell[9] and the structure determined from X-ray results, which is based in a pattern recognition approach to choose proper signs of the observed structure factors,[7,8] differ, however, in details regarding the form and size of the micellar aggregates, and specifically whether the two different categories occupying different special positions correspond to identical micelles with different rotational freedom or to actually different micellar forms.

There is not any theoretical model in the literature developed to explain the complete transition sequence I−Q^{223}−H. The mechanism of the Q^{223}−H phase transition was explained in terms of epitaxial relations within the two liquid crystal phases.[10] No mechanism for the I−Q^{223} phase transition has been yet proposed, but the presence of the Q^{223} phase has been associated to close packing of spheroidal micelles with molecular packing parameter $< 1/3$.[5,11]

In a previous work,[11] we determined the shape of the micellar aggregates in the I phase of the PLPC/water system, using small-angle X-ray scattering (SAXS) technique. The product $P(q)$-$S(q)$, where $P(q)$ is the micellar form factor and $S(q)$ is the intermicellar interference function calculated from a hard-sphere interaction potential, was modeled on the scattering curves. It was found that PLPC micelles remain with a prolate ellipsoidal shape of constant anisometry $\nu = 1.8$ in the whole concentrated I phase. The formation of the Q^{223} phase was discussed in terms of this result through the comparison with previous data obtained[12] in the study, by SAXS, of the I−H phase transition presented by the sodium dodecyl (lauryl) sulfate (SLS)/water system.

The direct I−H transition occurs because SLS micelles grow from ellipsoids to polydisperse spherocylinders (SC) in the concentrated I phase. PLPC micelles, instead, remain spheroidal[11] because of the smaller surfactant parameter value of PLPC molecules, as compared to that of the SLS molecule. The anisometry ($\nu \sim 1.8$) of the prolate ellipsoid in the I phase of the PLPC is in the limit that establishes[13] the prolate ellipsoid micellar conformation as more stable in the solution. For larger anisometries, the SC becomes more stable, in view of the bending elastic energy[13] of the polar/apolar interface. It was concluded that if two different micellar shapes (prolate + oblate) are present in the Q^{223} phase, there must occur a rearrangement of amphiphile at the phase transition. It was also concluded[11,13] that the oblate form is not present in the I phase.

In this work we analyze further the I−Q^{223} phase transition, performing X-ray scattering experiments in the low-concentration limit of the Q^{223} phase. Our aim is to get information on

10.1021/jp991940c CCC: $18.00
Published on Web 10/04/1999

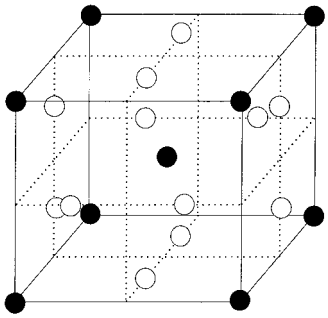

Figure 1. Q^{223} cubic phase structure:[5−9] full lines show the limits of the unit primitive cell. Broken lines are a guide for the eyes. According to X-ray scattering results,[7,8] the unit cell contains six discotic micelles (open circles) centered at the positions **c** ((1/4,1/2,0), (3/4,1/2,0), (1/2,0,1/4), (1/2,0,3/4), (0,1/4,1/2), (0,3/4,1/2)) and two spherical micelles (black circles) centered at the positions **a** ((0,0,0), (1/2,1/2,-1/2)). NMR results[5,6] are consistent with a model of spherocylindrical micelles both at **a** and **c** positions.

the mechanism of the phase transition, and specifically to test whether a single micellar form, as observed in the I phase, may remain in the Q^{223} phase.

II. Experimental Section

Aqueous solutions of PLPC with concentrations C ranging from 28 to 40 wt % of PLPC were prepared as previously described.[11] Isotropic samples with $28 \leq C \leq 37.5$ wt % of PLPC were conditioned in sealed 1 mm diameter glass capillaries, while 40 wt % of PLPC sample (cubic phase) was put in a sealed aluminum cell, of ∼1 mm width, with Mylar windows. Samples were investigated by X-ray scattering at room temperature 22 ± 1 °C with Cu Kα Ni filtered radiation, in the Laboratory of Crystallography of the Institute of Physics of the University of São Paulo. A punctual well-collimated incident beam was used. Data was collected on photographic film placed perpendicular to the incident beam to measure the radiation scattered by the sample; a sample−photograph distance of ∼10 cm was used in the Laue transmission geometry.

III. Results

Q^{223} Phase Study. The structure of the Q^{223} phase[5−9] is shown in Figure 1; there are 8 micelles in the primitive unit cell, 2 in position **a** and 6 in position **c** (2 in each face of the unit cell), with coordinates as stated in the figure caption.

We have studied the sample for 40 wt % of PLPC, near the I−Q^{223} phase transition. Table 1 shows the position of the measured diffraction peaks on the photographic film. We have also measured two additional peaks, not shown in Table 1, corresponding to the Mylar peak of the sample holder and to the water diffuse band near 4.5 Å.

Table 1 also shows the indexation of the diffraction peaks for our 40 wt % of PLPC sample compared with that obtained from previous X-ray experiments for a Debye−Scherrer spectra, collected using a Guinier camera for 50 and 41.8 wt % of PLPC.[1,14] Results referred to 40 wt % of PLPC show that it was not possible to differentiate between (2,1,0) and (2,1,1) reflections and between (2,2,2) and (3,2,0) reflections because Laue geometry did not provide enough resolution. It was also not possible to measure all the weaker reflections obtained with Guinier camera for 50 and 41.8 wt % of PLPC (corresponding to the smaller angles of scattering in the diffraction diagram), although we have observed reflections for higher values of the scattering vector. The dislocation of (3,2,1) reflection into (4,0,0)

TABLE 1: Comparison of the Q^{223} Phase Samples Indexation[a]

	C		
(h,k,l)	50 wt % PLPC $\lvert I\rvert$	41.8 wt % of PLPC s^{-1} (Å)	40 wt % of PLPC s^{-1} (Å)
(1,1,0)	3	−	−
(2,0,0)	33	68.6	−
(2,1,0)	290	62.9	
(2,1,1)	320	57.6	60.9 ± 2.6
(2,2,0)	20	−	−
(3,1,0)	7	−	−
(2,2,2)	55	−	
(3,2,0)	58	39	43.5 ± 1.7
(3,2,1)	96	37.4	−
(4,0,0)	33	−	36.7 ± 0.6
(4,1,0)	35	34.2	−
(3,2,2)			
(4,1,1)	36	−	−
(3,3,0)			
(4,2,1)	18	−	−
(4,4,0)	−	−	25.9 ± 0.1
(4,4,4)	−	−	21.0 ± 0.4
(8,1,1)			
(7,4,1)	−	−	17.9 ± 0.1
(5,5,4)			
(8,5,2)	−	−	15.1 ± 0.15
a (Å)	137	141	145.4 ± 1.4
$C_{v,par}$	0.272	0.249	0.216
$V_{p,T}$ (Å^3)	6.99×10^5	6.98×10^5	$(6.6 \pm 0.1) \times 10^5$

[a] Concentration C; indexes of the reflection (h,k,l); intensity of the reflection, $\lvert I\rvert$; scattering peak position s^{-1}; unit cell parameter a; paraffinic micellar volume $C_{v,par}$; and total paraffinic volume inside a unit cell $V_{p,T}$. Data for 50 and 41.8 wt % PLPC have been taken from refs 14 and 1. Reflections marked with (−) were not observed.

reflection is due to the difference in the water content of these samples. However, it is clear that the present results for 40 wt % of PLPC are consistent with data reported for Q^{223} phase.[1,14]

Table 1 shows that the cell parameter for 40 wt % of PLPC is $a = 145.4 \pm 1.4$ Å. According to this information, the distance between the micelles centered at the special positions **a** (Figure 1) is $d_a = 125.9 \pm 1.2$ Å.

The volume concentration of the paraffinic moiety is given by[15]

$$C_{v,par} = 0.57 \frac{1}{\left(1 + \frac{\upsilon_w(1-c)}{\upsilon_l \quad c}\right)} \tag{1}$$

where c is the weight concentration of PLPC in the sample, $\upsilon_l = 1.0585 \times 10^{-24}$ g/Å^3 is the specific weight of PLPC, and $\upsilon_w = 10^{-24}$ g/Å^3 is the specific weight of water. It is also possible to establish that

$$V_{p,T} = C_{v,par} a^3 \tag{2}$$

where $V_{p,T}$ is the total paraffinic volume inside the cubic cell.

$V_{p,T}$ can be calculated from equations 1 and 2, since the cell parameter a is experimentally measured. Table 1 shows $V_{p,T}$ values corresponding to 40, 41.8, and 50 wt % of PLPC. It is possible to conclude that the total paraffinic volume inside a unit cubic cell takes an approximately constant value $V_{p,T} \sim (6.9 \pm 0.1) \times 10^5$ Å^3 within the Q^{223} phase.

The total volume at 50 wt % of PLPC has been considered[7,8] to correspond to 2 spherical micelles in position **a** with paraffinic volume 55.0×10^3 Å^3 each and 6 anisotropic micelles in position **c** with paraffinic volume 87.5×10^3 Å^3 each, while at 41.8 wt % of PLPC the model[9] of 8 SC micelles with anisometry

TABLE 2: Indexation of the Reflections for 28 ≤ *C* ≤ 37.5 wt % PLPC According to a Local Cubic Symmetry[a]

C (wt % of PLPC)	N_p (micelles/Å^3)	s^{-1} (Å)	(*h*,*k*,*l*)	a_l (Å)	$\bar{a}_l$ (Å)	N_m
28	1.83×10^{-6}	67.7 ± 1	(2,0,0)	135.4 ± 2.0	134.0 ± 1.6	4.4 ± 0.2
		42.0 ± 0.3	(3,1,0)	132.7 ± 1.0		
30	1.96×10^{-6}	65.7 ± 2.1	(2,0,0)	131.4 ± 4.2	131.3 ± 2.5	4.4 ± 0.2
		41.5 ± 0.8	(3,1,0)	131.2 ± 2.5		
33	2.16×10^{-6}	64.5 ± 1.7	(2,0,0)	129.0 ± 3.4	129.4 ± 2	4.7 ± 0.2
		41.1 ± 0.7	(3,1,0)	129.9 ± 2.2		
35	2.29×10^{-6}	63.5 ± 2.2	(2,0,0)	127.0 ± 4.4	126.2 ± 2.3	4.6 ± 0.2
		39.6 ± 0.7	(3,1,0)	125.4 ± 1.4		
37.5	2.45×10^{-6}	62.0 ± 1.3	(2,0,0)	123.9 ± 2.7	124.4 ± 2.3	4.7 ± 0.3
		39.5 ± 1.2	(3,1,0)	124.9 ± 3.8		

[a] Concentration *C*; numeric density of micelles N_p; peak position s^{-1}; reflection indexes (*h*,*k*,*l*); local unit cell parameter a_l; mean value $\bar{a}_l$; and number of micelles per unit cell N_m.

of about 2 has been accepted. It should be pointed, however, that the method used to determine the different micellar volumes,[7,8] choosing an interface electron density level ρ_0 such that the total $V_{p,T}$ would be consistent with $C_{v,par}$, had as implicit hypothesis a constant paraffinic density in the enclosed volume. This method excluded therefore the possibility of different apparent micellar volumes due to different rotational freedom in the two positions, with a discotic shape for micelles in **c** (confined to hindered oscillations in a plane) and a spherical shape for the micelles in the cages around position **a**.

The possibility of different apparent volumes was not considered in refs 7 and 8 but also not eliminated by the structure determination. Note that the model of 8 identical micelles leads to apparent volumes larger for micelles in **a**, since the two forms have the same maximum dimension (see Figure 3 in ref 6), corresponding to electron density lower for the micelles in **a** than for the micelles in **c**. The hypothesis of constant density produces a volume in **a** smaller than it should, and that is precisely the result obtained in refs 7 and 8.

Keeping the model of 8 identical micelles,[9] our $V_{p,T}$ value corresponds to a micelle with a paraffinic volume of (86.0 ± 1.0) × 10^3 Å^3. The micellar volume of the prolate ellipsoidal micelles in the I phase[11] is (80.0 ± 2.2) × 10^3 Å^3. A small increase in micellar size may be occurring at the transition, possibly correlated to a change in form from prolate ellipsoid to SC, since the later form becomes energetically favored when the anisometry overpasses 1.8.[11,13]

Concentrated I Phase Study. Table 2 lists the scattering peaks measured by X-ray photograph for 28 ≤ *C* ≤ 37.5 wt % of PLPC. Note that the positions of these interference peaks do not exactly coincide with the peaks of the SAXS curves (Figures 6c and 7 of ref 11) because in that case the line focus produces a smearing effect. Here, with point focus, the peak positions can be interpreted as peaks of intermicellar interference.

If we interpret these two interference peaks in terms of a local positional order, it is possible to assign them as reflections in a crystal,[16] and to obtain the local cell parameter, for a given local symmetry.

The SLS/water system presents a direct I−H phase transition, and a local hexagonal order was found by one of us in the concentrated I phase of this system.[17] In the case of PLPC, we concluded after several tests that a local hexagonal order can be discarded. On the other hand, it is possible to obtain a satisfactory indexation assuming a local cubic symmetry.[16] Low-temperature EM results gave also evidence[18] of a local cubic order for 25 wt % of PLPC. Table 2 shows that s^{-1} values for 28 ≤ *C* ≤ 37.5 wt % of PLPC were indexed as (2,0,0) and (3,1,0) reflections. These reflections correspond to a local order of a cubic simple cell (a body-centered cubic cell cannot in fact be discarded).[16] The local cell parameter, a_l, of the simple cubic cell, obtained using (2,0,0) and (3,1,0) indices, are listed for each *C* in Table 2. The good quality of the indexation is shown by the small difference within the cell parameters determined from each scattering peak for a given *C*. Table 2 also shows the dependence of N_m, the number of micelles within the cubic Bravais lattice, with *C*. In our work, this parameter is given by

$$N_m = \bar{a}_l^{\,3} N_p \tag{3}$$

where $\bar{a}_l$ is the mean value between a_l parameters determined for each concentration between 28 ≤ *C* ≤ 37.5 wt % of PLPC. N_p, calculated from parameters determined in ref 11, is the number density of micelles, given by

$$N_p = \frac{3[\phi]N_a v}{4\pi v l_{par}^{\,3}} \tag{4}$$

where $N_a = 6.023 \times 10^{23}$ is the Avogadro number, $[\phi]$ is the molar concentration of the solution, and $v = 431$ Å^3 and $l_{par} = 22$ Å are the volume and the length of the paraffinic chain, respectively.

IV. Discussion

We have already indexed the scattering peaks at the concentrated I phase according to a local cubic symmetry. The next step is to show how this local order evolves to the liquid crystal phase. We must thus relate parameters on Table 2 with those corresponding to 40 wt % of PLPC, i.e., with those describing the liquid crystal Q^{223} phase.

$\bar{a}_l$ and N_m, listed on Table 2, can be extrapolated to 40 wt % of PLPC. Figure 2 shows such extrapolation, and that $\bar{a}_{l,ex} = 121.7 \pm 3.7$ Å and $N_{m,ex} = 4.8 \pm 0.7$ correspond to the extrapolated values of $\bar{a}_l$ and N_m.

It is thus possible to make a comparison between the results extrapolated from the I phase and those obtained in the liquid crystal phase at 40 wt % of PLPC.

In our previous work[11] we showed that PLPC micelles remain with a constant volume and anisometry for 5 ≤ *C* ≤ 37 wt % of PLPC. In this work (Table 2) we assume that this condition can be extended up to the beginning of the Q^{223} phase structure formation, i.e., at ∼40 wt % of PLPC.[1] This hypothesis leads to a total paraffinic value $V_{p,T} = 6.4 \times 10^5$ Å^3, which is of the order of the average value $V_{p,T} \sim 6.9 \times 10^5$ Å^3, determined before, within the Q^{223} phase.

By proportionality, $N_{m,ex}$ corresponds to a paraffinic volume $V_{p,ex} = (3.8 \pm 0.6) \times 10^5$ Å^3,[11] where the index ex has been used since this parameter is related to $N_{m,ex}$ and $\bar{a}_{l,ex}$.

Thus, the extrapolation of parameters on Table 2 to 40 wt % of PLPC together with the hypothesis that assumes the same micellar volume for 37.5 ≤ *C* ≤ 40 wt % of PLPC leads to the

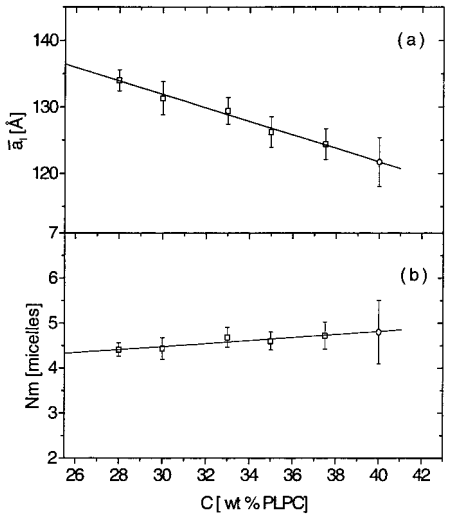

Figure 2. (a) (□) local cell parameter $\bar{a}_l$ listed on Table 2, extrapolated to 40 wt % of PLPC. (○) Extrapolated parameter $\bar{a}_{l,ex} = 121.7 \pm 3.7$ Å. (b) (□) number of micelles N_m per unit cubic cell with parameter $\bar{a}_l$ listed on Table 3, extrapolated to 40 wt % of PLPC. (○) Extrapolated parameter $N_{m,ex} = 4.8 \pm 0.7$.

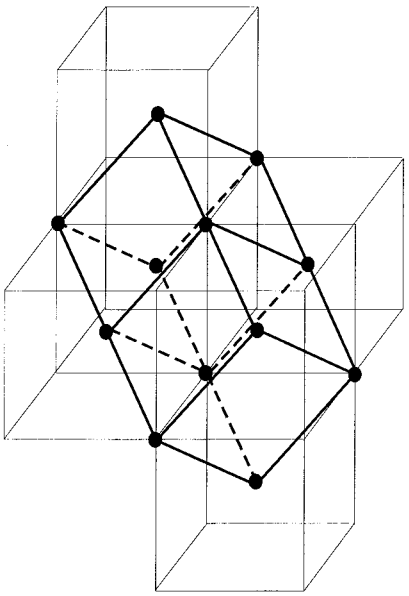

Figure 3. Full thin lines delimit six cells of the Q^{223} phase (Figure 1). Micelles centered at the special positions **c** of the spatial group *Pm*3*n* are not shown in order to simplify the picture (black circles correspond to micelles placed at the special positions **a** of the spatial group *Pm*3*n*). Full and broken heavy lines delimit two cubic cells with cell parameter d_a.

prediction of a net formed by cubic cells, characterized by $\bar{a}_{l,ex} = 121.7 \pm 3.7$ Å, $N_{m,ex} = 4.8 \pm 0.7$, and $V_{p,ex} = (3.8 \pm 0.6) \times 10^5$ Å^3.

Figure 3 shows six cells of the Q^{223} phase and two superposed cubic cells of parameter d_a. It is seen that the positions that form the cubic local cell of the I phase coincide with the special positions **a** of the Q^{223} unit cell. The parameter of the local cubic cell in the I phase coincides with the distance between the origin and the body-centered positions of the Q^{223} unit cell.

Also by proportionality, the paraffinic volume contained inside the cubic cell with parameter $d_a = 125.9 \pm 1.2$ Å is $V_{p,d_a} = (4.5 \pm 0.2) \times 10^5$ Å^3. According to the structure of the Q^{223} phase it is possible to conclude that for 40 wt % of PLPC, the cell with volume $V_{p,d_a} = (4.5 \pm 0.2) \times 10^5$ Å^3 contains $N_{m,d_a} = 5.2 \pm 0.3$ micelles.

TABLE 3: Comparison between the Parameters Corresponding to the Cubic Structures with Cells Parameters $\bar{a}_{l,ex}$ (Table 2, Figure 2) and d_a (Figure 3)[a]

	Q^{223} phase	extrapolated I phase
C (wt % of PLPC)	40	40
$C_{v,par}$	0.216	0.216
cell parameter	$d_a = 125.9 \pm 1.2$ Å	$\bar{a}_{l,ex} = 121.7 \pm 3.7$ Å
no. of micelles	$N_{p,d_a} = 5.2 \pm 0.3$	$N_{m,ex} = 4.8 \pm 0.7$
paraffinic volume	$V_{p,da} = (4.5 \pm 0.2) \times 10^5$ Å^3	$V_{p,ex} = (3.8 \pm 0.6) \times 10^5$ Å^3
Γ	0.225 ± 0.01	0.211 ± 0.04

[a] Concentration C; volume concentration of the paraffinic chains $C_{v,par}$; intermicellar distance, number of micelles inside the cells, total paraffinic volume inside the cells, and fraction Γ between the total paraffinic volume and the cell volume.

Table 3 compares the number of micelles and the total paraffinic volume inside each cell as well as the cell parameters, for cubic cells with d_a and $\bar{a}_{l,ex}$. Table 3 shows that there is a remarkable similarity between parameters corresponding to each class of cubic cell. The fraction between the paraffinic volume inside each cell, and the volume of the cell, Γ, is equal to $C_{v,par}$, showing the consistence of parameters on Table 3.

Data on Table 3 clearly suggests that the Q^{223} phase structure begins to be formed through the establishment of a net of cubic cells with parameter d_a, similar to that shown in Figure 3, superposed to the Q^{223} unitary cells. When C grows, the clusters with local cubic order at the concentrated I phase get closer in the solution. Each cluster is made by approximately 5 micelles, with positional correlations at a relative distance $\bar{a}_l$, which will correspond to the special **a** positions in the Q^{223} phase (Figure 1). Micelles within a cluster but at a distance smaller than $\bar{a}_l$ are still rather aleatory in the I phase, and specially do not have yet the strict restriction of moving in a defined plane, as they will have in the special **c** positions in the Q^{223} phase. Therefore, it is clear that micelles at a distance $\bar{a}_l$ within the local cubic cell in the concentrated I phase do not correspond to first neighbors. When the cell parameter of this local order reaches $\bar{a}_{l,ex} \sim d_a$, a long-range order is established in the solution because repulsive interactions compel the micelles within the cluster, which are the first neighbors of the micelles in **a**, to "freeze" in the special **c** positions. Thus, during the transition the number of neighbors in **c** as well as the degrees of freedom of rotation of the micelles are defined and the Q^{223} phase structure is formed.

In our previous study of the I phase,[11] we have shown that the I−Q^{223} transition occurs at volume concentrations comparable to the I−cubic transition expected for the packing of hard spheres.[19] It is shown here, however, that the process is somewhat more complicated.

The packing of hard spheres predicts[19] a transition to a face-centered cubic structure, with 4 spheres per unit cell. For PLPC molecules the micellar radius of a sphere with the same paraffinic volume as the anisotropic micelle, as well as the degrees of freedom of the PLPC molecules, lead instead to 5 micelles per local unit cell in the I phase and formation of a simple cubic cell with 8 micelles per unit cell in the Q^{223} phase.

It is also important to note that Γ in Table 3 is in good agreement with $C_{v,par}$ and that it was obtained, in the case of the extrapolated values, using the micellar shape determined in the concentrated I phase for PLPC.[11] This result suggests that PLPC micelles keep their integrity during the I−Q^{223} phase transition. But we cannot also discard the possibility of a change from prolate ellipsoidal to SC micellar shape with the same (or slightly larger) paraffinic volume just before or during the transition, possibly in the coexistence region, because SC

packing is easier than prolate ellipsoids packing, since the SC principal axis is shorter than prolate ellipsoids principal axis for a given paraffinic volume. It is not necessary, however, to postulate a complete rearrangement of molecules in aggregates of different (prolate + oblate) forms at the transition.

Acknowledgment. Financial support of FAPESP and PRONEX/CNPq/MCT is acknowledged. V.C. is grateful for a CNPq doctoral fellowship and FAPESP and CIES post-doctoral fellowships. The authors thank P. Mariani for helpful discussions.

References and Notes

(1) Arvidson, G.; Brentel, I.; Khan, A.; Lindblom, G.; Fontell, K. *Eur. J. Biochem.* **1985**, *152*, 753.

(2) Ekwall, P.; Mandel, L.; Fontell, K. *Mol. Cryst. Liq. Cryst.* **1969**, *8*, 157.

(3) Balmbra, R. R.; Clunie, J. S.; Goodman, J. F. *Nature (London)* **1969**, *222*, 1159.

(4) Tardieu, A.; Luzzati, V. *Biochim. Biophys. Acta* **1970**, *219*, 11.

(5) Eriksson, P. O.; Lindblom, G.; Arvidson, G. *J. Phys. Chem.* **1987**, *91*, 846.

(6) Eriksson, P. O.; Lindblom, G.; Arvidson, G. *J. Phys. Chem.* **1985**, *89*, 1050.

(7) Vargas, R.; Mariani, P.; Gulik, A.; Luzzati, V. *J. Mol. Biol.* **1992**, *225*, 137.

(8) Luzzati, V.; Vargas, R.; Mariani, P.; Gulik, A.; Delacroix, H. *J. Mol. Biol.* **1993**, *229*, 540.

(9) Fontell, K.; Fox, K.; Hansson, E. *Mol. Cryst. Liq. Cryst.* **1985**, *1*, 9.

(10) Mariani, P.; Amaral, L. Q.; Saturni, L.; Delacroix, H. *J. Phys. II (Fr.)* **1994**, *4*, 1393.

(11) Castelletto, V.; Itri, R.; Amaral, L. Q. *J. Chem. Phys.* **1997**, *107*, 638.

(12) Itri, R.; Amaral, L. Q. *Phys. Rev. E* **1993**, *47*, 2551.

(13) Taddei, G.; Amaral, L. Q. *J. Phys. Chem.* **1992**, *96*, 6102.

(14) Mariani, P.; Luzzati, V.; Delacroix, H. *J. Mol. Biol.* **1988**, *204*, 165.

(15) Gulik, A., et al. *J. Mol. Biol.* **1985**, *182*, 131.

(16) *International Tables for X-ray Cristallography*; The Kynoch Press: London, England, 1972.

(17) Itri, R.; Amaral, L. Q. *J. Phys. Chem.* **1990**, *94*, 219.

(18) Lindblom, G.; Rilfors, L. *Biochim. Biophys. Acta* **1989**, *988*, 221.

(19) Hoover, W. G.; Ree, F. H. *J. Chem. Phys.* **1968**, *49*, 3609. Pusey, P. N.; Megen, W. *Nature* **1986**, *320*, 340. Schaertl, W. *J. Stat. Phys.* **1995**, *79*, 299.